Study on Light Scattering Velocimetry by Using Ronchi-rulings

Masato FUNATSU[*1]; Kenji AMAGAI[*2]; Katsuine TABEI[*3]; Ryoko KAKINUMA[*4]

*1: Dept. of Mechanical Systems Engineering, Graduate School of Engineering, Gunma University, 1-5-1 Tenjin-cho, Kiryu, Gunma, JAPAN 376-8515, E-mail mfunatsu@gunma-u.ac.jp, Phone +81-277-30-1509
*2: Dept. of Mechanical Systems Engineering, Graduate School of Engineering, Gunma University, 1-5-1 Tenjin-cho, Kiryu, Gunma, JAPAN 376-8515, E-mail amagai@gunma-u.ac.jp, Phone +81-277-30-1513
*3: Past Affiliation; Dept. of Mechanical Systems Engineering, Graduate School of Engineering, Gunma University, 1-5-1 Tenjin-cho, Kiryu, Gunma, JAPAN 376-8515
*4: Dept. of Mechanical Systems Engineering, Graduate School of Engineering, Gunma University, (Present Affiliation; Atom Medical Corporation, 2-2-1 Doujoh, Sakura-ku, Saitama, Saitama, JAPAN 338-0835)

The Ronchi-ruling is a grating, with lines, spaces and small pitches of spatial frequency. This is used in a Ronchi test for the evaluation of surface flatness. In this study, a new type of velocimeter, using a Ronchi-ruling was proposed and its performances were investigated. When the stripes of laser light through a grid of the Ronchi-ruling illuminated the tracer particles moving with the flow, the scattered light signal could be obtained as a wavy signal of light intensity. This signal was detected by a photomultiplier. Frequencies of the obtained signal were measured by an FFT analyzer. The flow velocity was calculated from the grid pitch and the frequency. This method was applied to the measurement of velocity profiles of pipe flows. The profiles measured by this velocimeter agreed with theoretical profiles of the laminar and turbulent flows.

1. Introduction

An optical element called Ronchi-ruling[1, 2)] is widely used for the evaluation of the resolution of optical system, the check of accuracy of lens surface, the measurement of object surface flatness by still patterns, and the measurement of object size and the displacement by shifted moiré patterns. Ronchi-ruling is a grating in which straight lines and spaces are alternately allocated at even intervals. In the past, a technique to measure the traverse speed of object has been proposed, in which the Ronchi-ruling is set between a moving object and a detector[3, 4)]. However, since the above method observes the object through the Ronchi-ruling, the detection of the measurement point in the depth direction is fairly difficult. Therefore it is not suitable for the velocity measurement in the general flow fields.

In this paper, a new method of the flow speed measurement is proposed in which a laser beam is irradiated through Ronchi-ruling and a stripe of the light is formed in the space. The stripe of the light generated in the space has the same wave length as the pitch of Ronchi-ruling. When a tracer particle moving with the flow passes through the light-stripe formed in the flow field, a periodic scattered light can be observed, and it is possible to obtain the speed of the particle by capturing the scattered light. This method is considered to be similar to the conventional representative velocimeter LDV (Laser Doppler Velocimeter)[5-8)] and L2FV [9)] in which the particle speed is measured from the transit time lag of the signal between two laser beams.

The principle of the present measurement is different from the LDV method in the following points. That is, LDV uses the light-interference fringe formed at the crossing point of two laser beams but the present method uses the light stripe made by only one light beam and Ronchi-ruling. Such a velocimeter can be expected to apply to the hydraulic model experiment of the ocean current and the flow around a ship in a water tank, and also to the multiphase flow in the pipeline and the flue dust monitoring within the gas duct. In these flows, the local

Translated from Journal of the JIME Vol.44, No.1 ©2009(Original Japanese)

instantaneous flow measurement as the turbulent factor is not necessarily required, while a quick measurement is preferable. Moreover, the present method is adapted to the simple speed measurement for education and studies since the method is possible to measure the lower speed than the measurement by Pitot tube.

In this study, we clarified a basic concept of the measurement method using Ronchi-ruling and examined applicability to the real flow field.

2. Principle of measurement

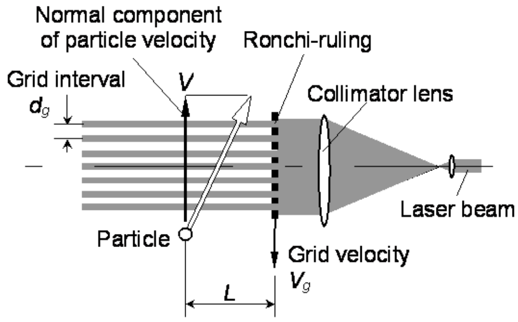

Fig. 1 Principle of Ronchi-ruling velocimeter

Figure 1 shows the measurement principle of the flow velocimeter proposed in this study. A source of light is the parallel ray such as a laser beam. A stripe of the light is formed in space by irradiating the rays in Ronchi-ruling, where grid interval d_g equals to the pitch of the stripe. Generally the diffraction phenomenon occurs when light passes a grid such as Ronchi-ruling. The diffracted light is accompanied by the first order, the second order, and higher order diffractions. These high order diffractions spread obliquely and widely, in effect obscuring the clearness of the light-stripe region. However, the light-stripe becomes clear at the position where the higher diffraction light just intersects the light-stripe after passing the grid. Based on Talbot's condition[10, 11], the distance L from the grating that the light-stripe becomes clear is expressed by

$$L = \frac{d_g^{\ 2}}{\lambda}(N - s) \quad \sim \quad \frac{d_g^{\ 2}}{\lambda}(N + s), \tag{1}$$

where λ is the wave length of transmitted light, N (= 0, 1, 2, 3, ···) the order number of the interference, and s the value which should be determined experimentally for the clear light-stripe. From a preliminary experiment, when the value s is 0.25, a fairly good light-stripe can be obtained. In order to measure the flow velocity, we must put the measurement object at the position satisfying the Talbot's condition. The speed can be calculated from the frequency of the scattered light of tracer particles passing there.

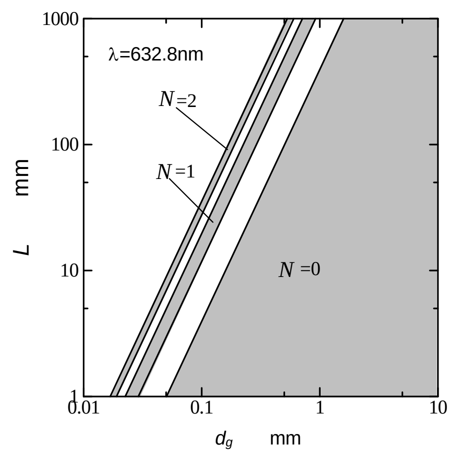

Fig. 2 Relationship between L and d_g

Figure 2 shows the measurement range L calculated from Eq. (1) for the He-Ne laser of wavelength λ=632.8 nm. The length L for the clear appearance of light-stripe becomes large, as d_g increases. This means that the present device is suitable for the measurement of the bubble flow and the massive mist flow including comparatively large droplet over 0.1 mm in diameter. Now, we consider the case that the particle passes within the space formed by the light-stripe with a certain speed. The frequency of scattered light of the particle f [Hz] is given by

$$f = \frac{V}{d_g}, \tag{2}$$

where V is the normal velocity component of the passing tracer particle against the light-stripe. In order to apply it to the case that the particle velocity is very slow or the passing direction of the particle is unknown, the grid of Ronchi-ruling should be moved at a constant speed. As shown in Fig. 1, when the motion direction of the particle is reverse to the transfer direction of the light-stripe, Eq. (2) is rewritten as

$$f = \frac{V + V_g}{d_g}, \tag{3}$$

where the movement speed of the grid is V_g. Since the V_g and d_g are known values, the velocity V of particle passing the light-stripes can be obtained from the frequency f of the scattered light signal. In case of f larger than f_g (= V_g / d_g: the shift-frequency), it means that the particle moves reversely with the movement direction of the grid. Conversely, in case of f smaller than f_g, it means that the particle moves in the same direction as the movement of the grid. The present device has characteristics that the grating pitch d_g can be chosen freely, and that the measurement space (the sampling volume) can be restricted freely by adjusting the image lens and the aperture.

The space distance L_s which is necessary for the measurement is supposed to be about 3 times of the pitch d_g. Hence the time resolution T is estimated from the particle speed V and the frequency f, as follows.

$$T = 1 / f = L_s / V = 3\, d_g / V \tag{4}$$

For example, since the length of d_g is 0.1 mm for Ronchi-ruling of 250 lines per 1 inch, the values are calculated as T=30 ms, f=30 Hz in the case of V=10 mm/s, and T=3 ms, f=300 Hz in the case of V=100 mm/s. Accordingly we can measure the flow speed for steady flow or periodic flow with the above time interval T.

3. Experimental apparatus and method

In order to confirm whether the flow velocity could be really measured based on the principle mentioned above, we took up the most basic circular pipe flow and constituted the experimental device as shown in Fig. 3. The device consists of the circular pipe, the generation system of the stripe rays by Ronchi-ruling with a laser, and the detector of the scattered light signal. The flow duct is an acrylic pipe of 26 mm inside diameter, 30 mm outside diameter, and the inlet length to the measurement point is 1,000 mm. The fluid is tap water with a pump circulation. The average flow velocity in the pipe was changed in the range of 0 ~ 350 mm/s, of which Reynolds number corresponded to 0 ~ about 9,000. Therefore, the condition of the flow in the pipe varied from the laminar flow to the turbulence flow. In addition, to reduce the influence of the refractive index of the transparent acrylic pipe as much as possible, a rectangular water jacket was adapted around the pipe.

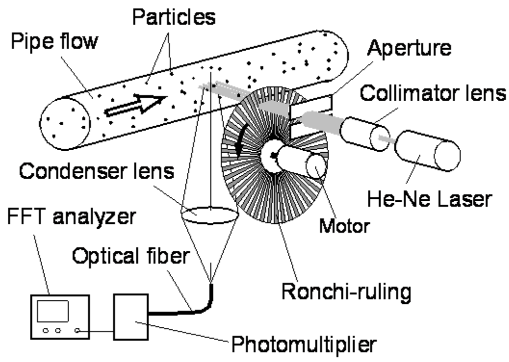

Fig. 3 Schematic view of experimental apparatus

As the tracer particle for light scattering, we used two kinds of particles. One is a polystyrene particle of specific gravity 1.06, the average particle size 379 μm, and the other is a nylon particle of Nylon12 of specific gravity 1.02, the average particle size 310 μm. It is said that the polystyrene particle follows the change of the flow of 200 Hz with the decrement speed of about 1% [12]. Furthermore the sedimentation speed of the particle was estimated to be about 1.5 mm/s. So we could use it substantially as the tracer particle of this measurement. The addition of particles into the water was adjusted in order to accurately detect the scattered signal. From the result of preliminary experiment, the suitable particle number density was decided as $36 \times 10^6 / m^3$.

As a light source to form the light-stripe in a flow field, the He-Ne laser (Melles Griot Co., 05-LHP-151, 5mW) was used. The laser beam having a diameter of 10 mm just behind a collimator was more narrowed to the sheet rays of 2.0 mm width by the aperture of a slit type. This sheet rays were irradiated to the central axis of circular pipe. The intensity distribution of the laser beam would not be always uniform, but we did not correct it in particular. The sheet ray passes a rotary grid (Ronchi-ruling) as shown in Figs. 1 and 3, where the light-stripe moves in the reverse direction against the pipe flow. The rotation grid (720 lines/360°) is the disc in which the grid clearance changes in the radial direction. In this case we would regard the radial grating in approximation to the parallel grid, by setting the passage position of rays at a fairly large radius. The radial position where the ray illuminated the disc was r_g=83 mm, and at this position the grid pitch was 0.922 mm per a line pair (the length lp regarded the pitch including the light and shade portion of the grid as one pair).

Figure 4 is a photograph of the scattered light of the particle in the illuminated area (the picture is enlarged and the exposure time is about 0.5 *s*). The particle moves toward right with the carrying flow. When a particle passes through the light-stripe by Ronchi-ruling, the light scattering occurs, and it is observed as a sequential dots line. The scattered light from the particles is concentrated by a condenser lens, and led to the entrance of the optical fiber. The intensity of scattered light is converted to a voltage signal by the photomultiplier placed at the other end of the optical fiber. The size of the spatial region detected by a condenser lens was about 4.0 mm in the flow direction, and 1.5-2 mm in the radial direction. The width of the beam changed in every radial position from the wall side to the pipe center due to the refraction effect of the acrylic pipe. Since the thickness of the sheet light was 2.0 mm, the measurement volume of this device was 1.5-2.0 mm height, 2.0 mm depth and 4.0 mm width. Therefore it is supposed that four or five stripes are contained within the measurement volume judging from the grid interval of Ronchi-ruling. The frequency spectrum of the scattering signal was measured by FFT analyzer (Ono Sokki Co., CF-350Z).

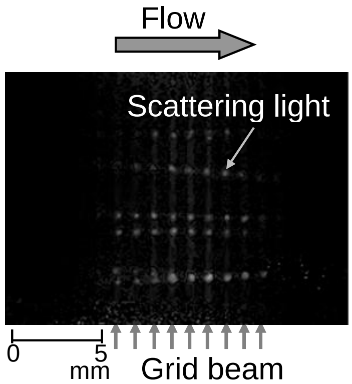

Fig. 4 Scattering image of tracer particles

The equation (3) can be transformed as follows.

$$f = \frac{V + r_g \omega_g}{d_g}, \tag{5}$$

where ω_g is the angular rotation speed of the grating disc, r_g the radius at the position where the light irradiates on the disc. In this case the shift frequency is given by $f_g=(n_g\omega_g)/2\pi$ in which n_g is the total number of grid lines of the disc. Therefore, the speed V is expressed as the next.

$$V = \frac{2\pi r_g}{n_g}(f - f_g) \tag{6}$$

If the frequency f is given by the scattered signal, the speed V can be calculated by using the known shift frequency.

Figure 5 shows an example of the frequency spectra measured by FFT analyzer. One is the spectrum of the scattered light signal obtained by fixing a grid in the space, and the other one is the spectrum for the moving grid. The low frequency component less than 0.1 kHz is regarded as the signal component due to the disc rotation which is unnecessary in this measurement. The frequency component of the scattered light signal in the case of a fixed grid appears at the position of (a) (heavy solid lines). Though the frequency component showed the band spectrum having some width, the frequency of the highest peak was assumed to be the value f in Eq. (6). The thin solid line indicates the spectrum in case of the moving grid. The peak (b) of this spectrum corresponds to the shift frequency f_g , so the value of f_g can be found from the spectrum even if the movement speed of the grid is unknown. The peak of (c) expresses the frequency component of the scattered light signal of f. In this example, the values of the peak of (b) and (c) are f_g=727 Hz and f=1,185 Hz, respectively. Accordingly the speed is calculated as V=0.33 mm/s from Eq. (6).

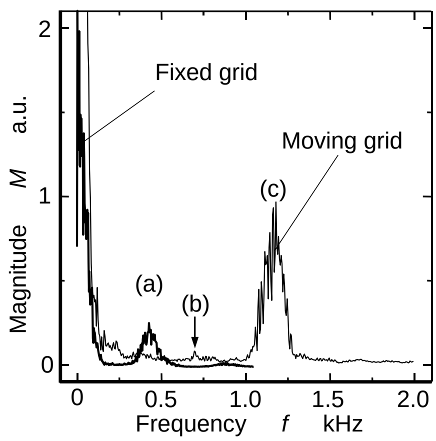

Fig. 5 Frequency spectra of scattering light

The speed measurement error $\Delta V/V$ in this method is considered to depend upon the dimension error of the light-stripe formed within the space and upon the error of the frequency of scattering light. That is,

$$\frac{\Delta V}{V} = \frac{\Delta d_g}{d_g} + \frac{\Delta f}{f}, \qquad (7)$$

where the first term in the right-hand side is the error of the grid stripe and the second term is the error of the frequency measurement. The error of the grid pattern prepared this time was around 10%. The measurement resolving power of the FFT analyzer was 0.0025 times of the setting frequency range. Assuming that measurement frequency was a half of the setting frequency range, we could estimate the frequency measurement error as about 0.5%. Hence the total error of the experimental device was regarded as around 11%. The measurement accuracy, however, may be improved more if we can utilize a precise grid by the etching process.

4. Experimental results and discussion

4.1 Confirmatory experiment with high-speed video

In order to confirm whether or not we could measure flow velocity by the principle mentioned above, the speed derived from the scattered signal was compared with the speed detected by high-speed video camera. In the confirmatory experiment, the droplet of the water mist (droplet diameter 60-300 μm) was used as the scattering particle, because it was very convenient to take a picture by the video camera. Figure 6 shows the resultant diagram. The horizontal axis indicates the injection pressure of the mist jet. The symbol ● in the figure is the speed from the high-speed video, and the symbol ○ is the speed from the scattering method. It can be seen that both are agreeable.

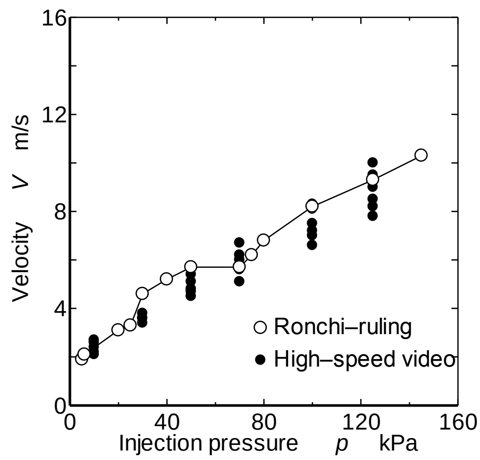

Fig. 6 Result of confirmatory experiment with high-speed video

4.2 Relationship between grid interval and particle diameter

Next, the experiment for the pipe flow shown in the experimental device was performed.

In order to know which grid clearance is suitable for the measurement, the scattered signal was observed by changing the grid clearance of Ronchi-ruling. As previously described, the average scattered particle size used in this study was 379 μm and 310 μm. Figure 7 shows the wave pattern of the scattered signal obtained for three grid spacing of 2.959 mm/lp, 0.922 mm/lp, and 0.253 mm/lp, respectively. The actual light beam size is a half of the above value because the line pair consists of one set of light and shade. Though the electric circuit had the characteristic that the voltage signal decreased when the scattering signal was detected, it was no problem for the frequency analysis.

From the experimental result, when the grid spacing was very large compared with the particle diameter as d_g=2.959 mm/lp, the clear periodic waveform could not be seen, but in cases of 0.922 mm/lp and 0.253 mm/lp, we could see the periodic wave pattern. In the case of 0.253 mm/lp in particular, it was confirmed that the periodic scattered signal occurred as expected though the average particle size was larger than the grid clearance. In this case each peak of the wave pattern stays in the negative region and did not return to the value of 0 V. It is caused by that the plural rays are scattered at the same time since the scattering particle is larger than the interval of rays. When plural particles exist in the sampling volume, the influence on peak frequency by FFT is considered to be slight, if the movement of the particles is the same.

Figure 8 shows the frequency spectra obtained in the same condition as Fig. 7. The frequency more than 1 kHz is not displayed by the measurement range setting in case of d_g=2.959 mm/lp and 0.922 mm/lp. From the figure, it can be found that the clearest peak appears in case of 0.922 mm/lp. That is because the periodic scattered signal has a fairly good periodicity when the width of rays formed by Ronchi-ruling is a little wider than the average particle size. Therefore, the grid spacing of 0.922 mm/lp was adopted in the following experiments.

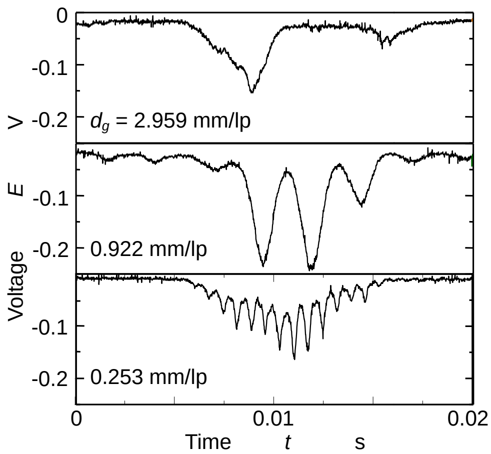

Fig. 7 Burst signal of scattering light

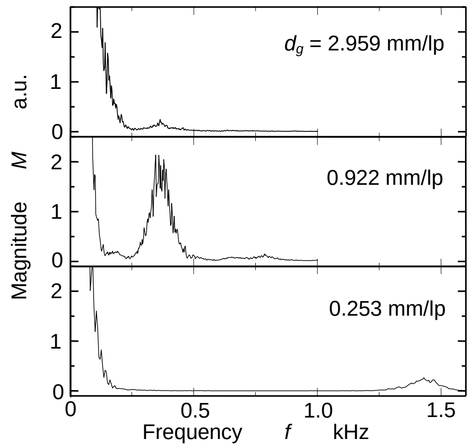

Fig. 8 Frequency spectra of scattering light at various grating spaces

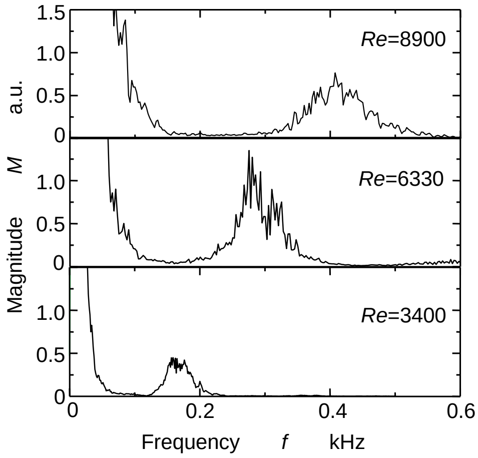

Fig. 9 Frequency spectra of scattering light at various Reynolds numbers

4.3 Measurement of pipe flow

For the center flow of the pipe we examined how the frequency spectrum changes when the speed changes. Figure 9 shows spectrum examples measured on the axis of the pipe for Reynolds number *Re* =3,400, 6,330 and 8,900, respectively. The flow condition of *Re* =3,400 is the transition flow and the others are the turbulent flow. The spectra show the band shape due to the scattering signal in every case but we can find the peak value. With the increase of the Reynolds number, the width of the band spectrum also widens. This is because the change of the particle speed becomes large with the increasing of the fluctuation of turbulent flow.

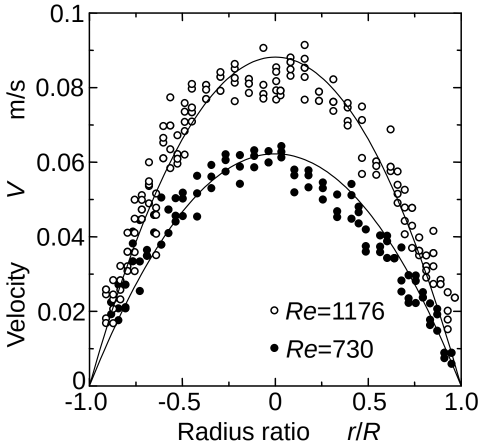

Fig. 10 Velocity profiles of laminar pipe flows

Figure 10 is the result of the velocity distribution of the pipe flow measured in the laminar flow condition (*Re* =730 and 1,176). The solid lines express the theoretical distribution for laminar flow developed sufficiently within the entrance region. In each Reynolds number, it was found that the measured velocity distribution agreed well with the theoretical distribution. In addition, we could measure the slow velocity near the wall less than 0.01 m/s, which was generally difficult to detect in the Pitot tube measurement. The fluctuation of each position of the measurement data is due to the both the small turbulence component which also exists within the laminar flow, as well as the reading errors of the peak wavelength from the frequency spectrum.

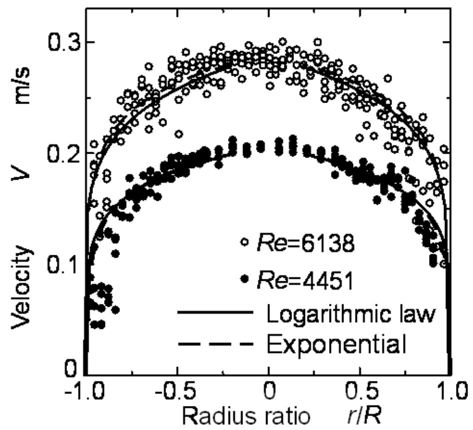

Fig. 11 Velocity profiles of turbulent pipe flows

Figure 11 shows the measurement result in the turbulent flow condition of *Re* =4,451 and 6,138. The solid line is the average velocity distribution calculated from the expression of the logarithm law for the smooth pipe flow, and the broken line is the distribution calculated from the 1/7 power law. The both of velocity distribution by the logarithmic law and by the 1/7 power law takes almost the same value, so the solid line and broken line overlaps. In comparison of an experiment result and the theoretical distribution, we can see that both agree well in each Reynolds number condition. The variation of the data at each position seems to depend mainly upon the fluctuation by the turbulence and the reading error of the peak of the frequency spectrum. In comparison with Figs. 10 and 11, the degree of the change for the averaged velocity is almost the same relatively, but the absolute value of the fluctuation for the turbulent flow is larger than that for the laminar flow.

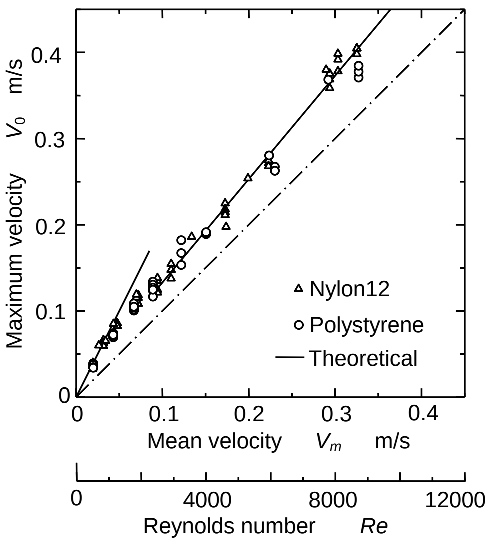

Fig. 12 Relationship between mean velocity and maximum velocity

In Fig. 12 the maximum flow velocity on the tube central axis is plotted against the mean velocity derived from the flow rate. Solid lines are the relationship between the mean velocity and the central speed, which is deduced from the semi-theoretical formula of laminar flow and turbulent flow mentioned above. It is found that the experimental velocities agree with these lines well. From the above fact, it is confirmed that the velocity measurement of flow field is possible by the presented measurement method using Ronchi-ruling.

5. Conclusions

Using the measurement method by Ronchi-ruling which is a straight grid having the same width of spacing, the flow velocity was measured, and the following conclusions were derived.

(1) The speed of the flow could be measured by detecting the scattered light signal from the fine particles passing through a stripe of light produced in space by Ronchi-ruling.
(2) The clear scattered light signal could be detected when the width of striped light is slightly wider than the diameter of tracer particles.
(3) By applying this measurement method to a laminar flow and a turbulence flow in the circular pipe, we could obtain the averaged velocity distribution.

Acknowledgments

The authors were given support from JST Satellite Niigata (Independent corporation) "Experimental research for the discovery of seeds in 2006" as a part of the development expense of the experimental device on performing this study. In addition, school’s students, So, S., Takahashi, T. and Mochizuki, S. volunteered to assist. Here we send our deep appreciation for them.

References

1) Tsuruta, T., Applied Optics I, (1990), p.266, Baifukan, *in Japanese*.
2) Mashima, M. and Isobe, T., Outline of Method of Measurement, (1991), p.66-68, University of Tokyo Press, *in Japanese*.
3) Shaklan, S., Pravdo, S., Gatewood, G., and Ftaclas, C., Modeling of a Space-based Ronchi-ruling Experiment for High-precision Astrometry, Astrophysics and Space Science, Vol.212, No.1-2, (1994), pp. 453-463.
4) Borders, J. L. and Granger, H. J., An Optical Doppler Intravital Velocimeter, Microvasc Res. Vol.27, No.1, (1984), pp.117-127.
5) Maeda, M. and Hishida, K., Sizing and Velocity Measurement of Particles in Spray Jet Using a Two-Colour, Four-Beam LDV, Laser Diagnostics and Modeling of Combustion, (1987), pp.1-10.
6) Obokata, T. and Hanada, N., Gas Velocity and Turbulence Measurement in a Spark Ignition Engine Using a LDA with a Fiber-Optic Pick-Up, Laser Diagnostics and Modeling of Combustion, (1987), pp.251-258.
7) Obokata, T. and Oosawa, T., Laser Measurement, (1994), p.105, Shokabo Publishing, *in Japanese*.
8) Nakatani, N., Yamada, T. and Sakabe, T., Measurement of Turbulent Structure in Premixed Flame with Multi-point LDVs, Laser Diagnostics and Modeling of Combustion, (1987), pp.11-20.
9) Hayami, H. and Hirashima, K., Velocity Measurement in Combustion Fields Using a Laser-2-Focus Velocimeter, Laser Diagnostics and Modeling of Combustion, (1987), pp.21-28.
10) Glatt, I. and Kafri, O., Moire-deflectometry (Ray Tracing Interferometry), Optics and Laser in Engineering, Vol.8 (1988), pp.277-320.
11) Ovchinnikov, Y. B., Fresnel interference pattern of triple-slit interferometer, Optics Communications, Vol.216 (2003), pp.33-40.
12) The Visualization Society of Japan, Handbook of Particle Image Velocimetry, (2005), p.31, Morikita Publishing, *in Japanese*.